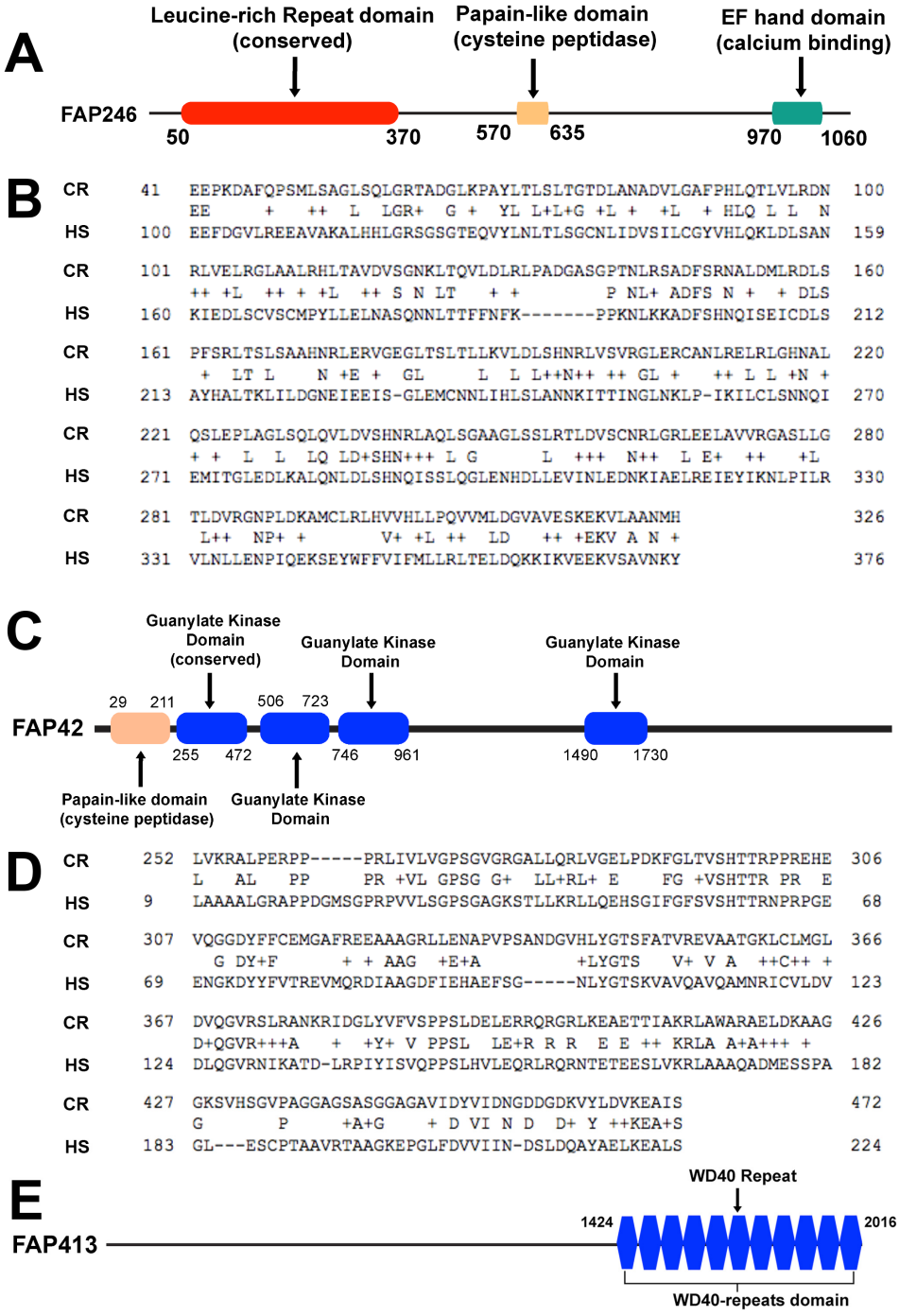

Fig. S1. Protein domain predictions and sequence alignments. **A-E)** Domain predictions for FAP246 (**A**), FAP42 (**C**) and FAP413 (**E**), and sequence alignments of FAP246 (**B**) and FAP42 (**D**) with the human proteins LRGUK-1 (NP_653249) and GUK1 (NP_000849-1) respectively. CR, *Chlamydomonas reinhardtii*; HS, *Homo sapiens*.

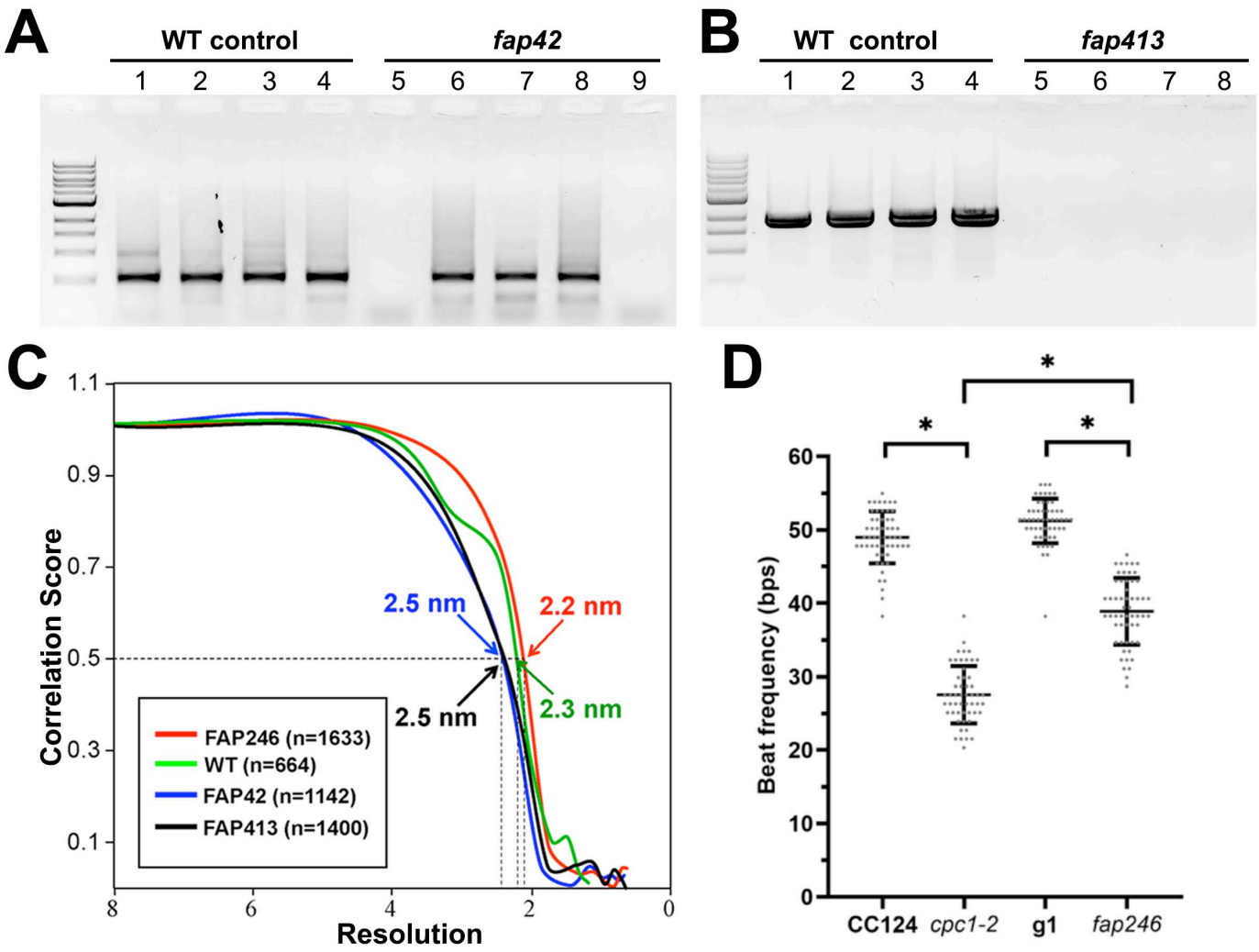

Fig. S2. Genotyping, resolution estimation and beat frequency analyses of various C1b mutants. **A-B)** Genotype analyses of the *Chlamydomonas fap42* and *fap413* CliP mutant strains. Lanes 1-4 in both **A**) and **B**) are PCR results of four WT control *Chlamydomonas* colonies, all showing an amplification product of expected size. Lanes 5-9 in (**A**) are the PCR results of five different *fap42* colonies, revealing genetic heterogeneity in the original CLiP cell line. Clones analyzed in mutant lanes 5 and 9 lack the amplification product, confirming disruption of the *FAP42* gene by the insertion cassette in these two clones. The clone of lane 5 was named "*fap42- 1*" and used for further experiments. The primer sets listed in Table S4 were used for both WT control and *fap42* PCR experiments. Lanes 5-8 in (**B**) are the PCR results of four different *fap413* colonies, all showing lack of the amplification product. The clone of lane 5 was named *fap413-1* and used for downstream

experiments. **C)** Fourier Shell Correlation (FSC) curves of the CA averages of WT (green), *fap246* (red), *fap42* (blue) and *fap413* (black) axonemes show that the resolutions are estimated to be 2.3 nm, 2.2 nm, 2.5 nm and 2.5 nm (0.5 criterion), respectively. **D)** Scatterplots showing flagellar beat frequencies of *cpc1* and *fap246* mutants and their respective parental strains CC-124 and g1. For each strain, the solid bars show mean and standard deviation. Significant differences (Student's t test, $P<0.01$) between strains are indicated by *.

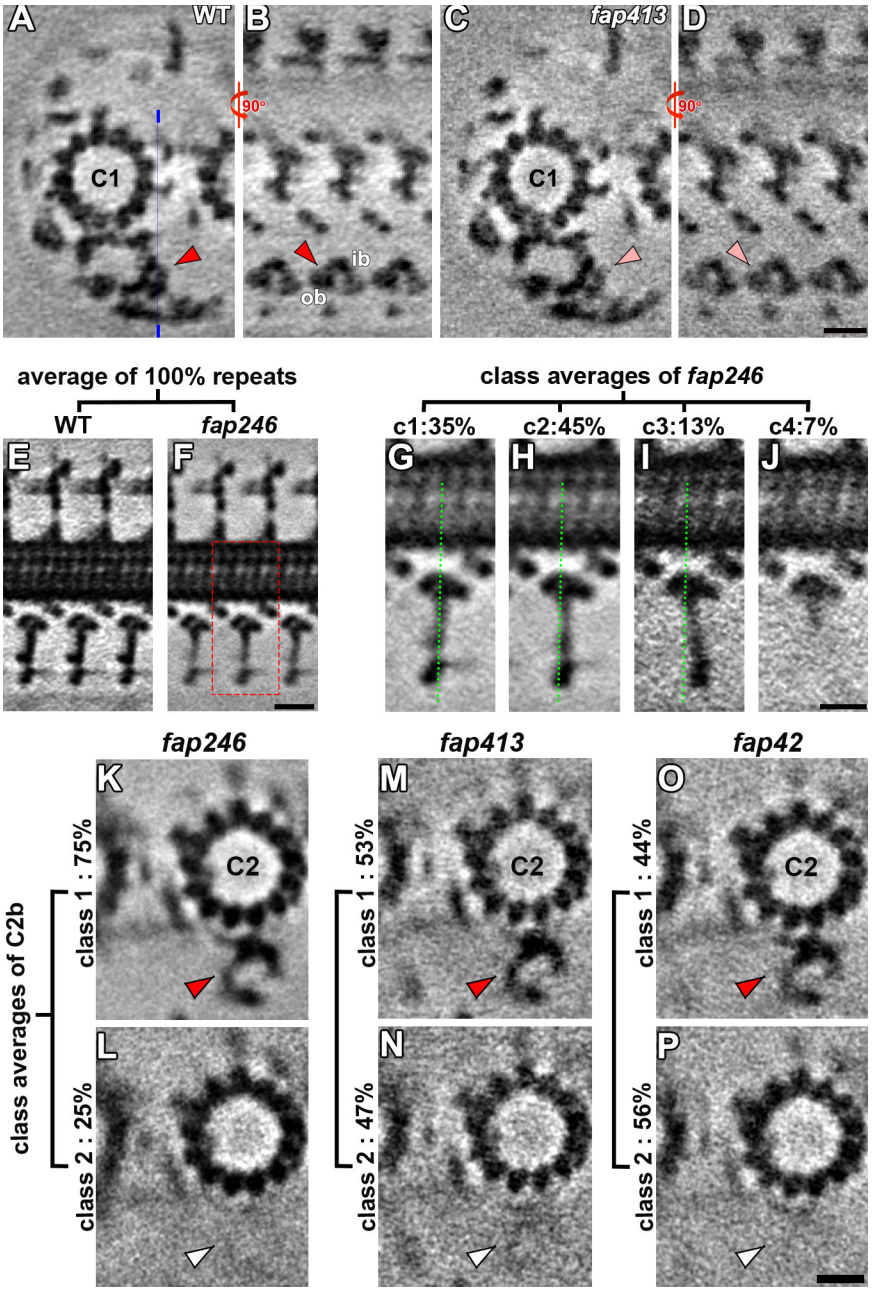

Fig. S3. Cryo-ET and subtomogram averaging localized FAP413 to the C1b projection, classification analyses of the pillar density of the *fap246* CA revealed positional flexibility, and classification analyses of the CA of all three C1b mutants revealed partial loss of the C2b density. A-D) Tomographic slices of the averaged CA repeats of WT (**A** and **B**) and *fap413* (**C** and **D**) in cross-sectional (**A** and **C**) and longitudinal views (**B** and **D**) show that the outer bracket (ob) density is fully present in the wild-type CA (red arrowheads) but significantly weakened in *fap413* (pink arrowheads). The thin blue line in (**A**) indicates the locations for the

slices shown in (**B** and **D**). Other labels: ib, inner bracket. Scale bar: 10 nm (in **D** valid for **A**-**D**). **E**-**J**) Classification analyses revealed structural heterogeneity in the *fap246* but not the WT C1b projection. Longitudinal tomographic slices of the averages that included all CA repeats showed that the pillar density was blurred in the *fap246* mutant (**F**) compared to WT (**E**). Classification analyses focused on the pillar density revealed four distinct classes (percentages of repeats are indicated for each class) (**G**-**J**). The regions shown in (**G**-**J**) are indicated by the red dotted box in (**F**). The green dotted lines serve as references to show the positional differences between classes. Scale bars: 10 nm (in **F** valid for **E** and **F**); 5 nm (in **J** valid for **G**-**J**). **K**-**P**) Classification analyses focused on the C2b density of the CA averages of *fap246* (**K**-**L**), *fap413* (**M**-**N**) and *fap42* (**O**-**P**) all revealed two distinct classes (percentages of repeats are indicated for each class). In the cross-sectional views for each mutant, the density is present (red arrowheads) in class 1 and missing (white arrowheads) in class 2. Scale bars: 10 nm (in **P** valid for **K**-**P**).

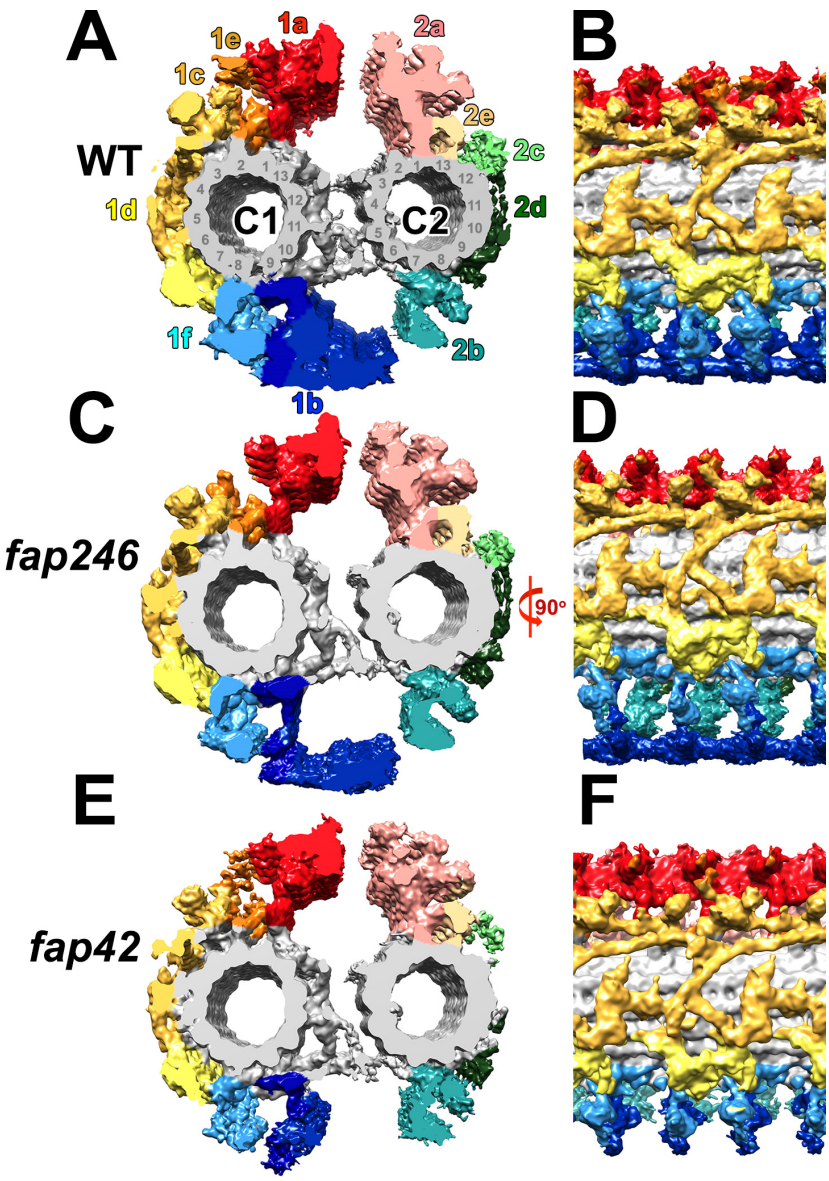

Fig. S4. Averaged CA repeats of WT, *fap246* and fap42 revealed structural defects of the indicated mutants. A-F) Isosurface renderings showing the *entire* averaged CA repeats (as compared to partial views in various main figures) of WT (**A** and **B**), *fap246* (**C** and **D**), and *fap42* (**E-F**) viewed in cross-sectional (**A**, **C** and **E**) and longitudinal orientations (**B**, **D** and **F**).

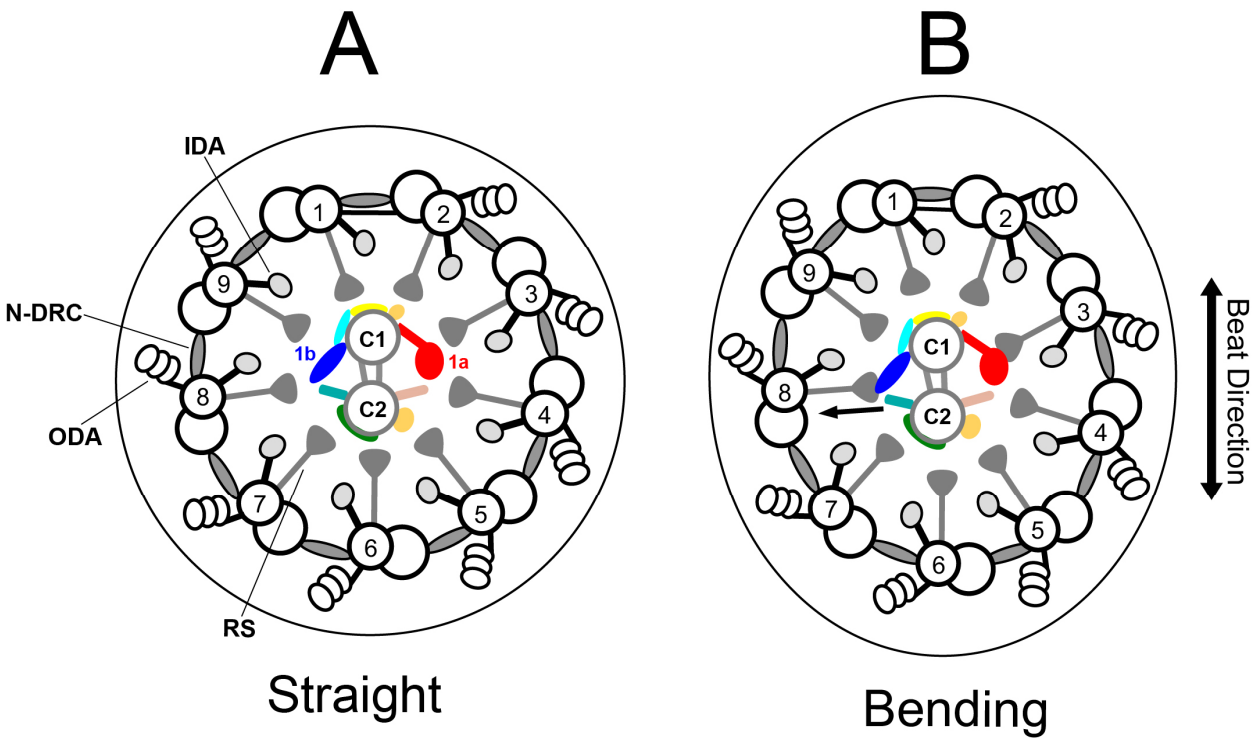

Fig. S5. Model depicting how the C1b projection may resist compression force during axonemal bending and how CA-RS mechano-signaling may transmit signals to regulate dynein activity and ciliary motility. A) In a straight flagellum, the 9 DMTs of the axoneme are cylindrically arranged around the CA, and all RS heads are equally distant from the circumference of the CA, i.e. the outermost periphery of the CA projections. **B)** In bent regions of a *Chlamydomonas* flagellum, the C1 and C2 microtubules are both in the plane of bend and, at least in the principal bend, C1 is on the outside of the bend, facing DMT 1 (Mitchell, 2003). When the flagellum bends, the axoneme becomes wider in the plane of bend (Lindemann and Mitchell, 2007), causing the RS heads to mechanically push against the C1a (red) and C2a (pink) projections on one side of the CA and the C1b (dark blue) and C2b (light green) projections on the opposite side. The pillar-bracket-beam structure of the C1b projection provides structural stability that likely resists this mechanical force (arrow). This mechanical interaction between the CA and RSs also could play a role in transmitting signals that regulate dynein activity and thus ciliary beating. In both panels, the axoneme is viewed from inside the cell. DMTs are numbered according to (Hoops and Witman, 1983); the black line between DMTs 1 and 2 represents the peripheral link between these two DMTs.

Table S1. MS/MS analyses of the axonemes of the *fap246*, *fap413* and *fap42* mutants — CA proteins assigned to C1a, C1c, C1d, C1e and C2b, or that were not previously confirmed to be components of a specific CA projection.

Protein	CA projection	Phytozome gene number	MW (kDa)	No. of Unique Peptides				Quantification Ratio		
				WT	*fap*246	*fap413*	*fap42*	*fap*246/WT	*fap42*/WT	*fap*413/WT
CA proteins[a]										
FAP54	C1d	Cre12.g518550	319	121	127	121	125	1.05	1.13	0.99
FAP46	C1d	Cre10.g420800	291	123	124	123	126	1.00	1.10	1.00
FAP221	C1d	Cre11.g476376	71	25	24	22	24	0.95	1.04	0.67
FAP297	C1d	Cre01.g029350	74	41	41	41	43	0.92	0.96	0.94
FAP74	C1d	Cre06.g271150	200	64	66	66	67	1.07	1.17	1.05
PF6	C1a	Cre10.g434400	237	100	104	107	107	1.11	1.05	1.05
PF16	C1a	Cre09.g394251	50	26	25	29	24	0.97	0.91	1.08
FAP92	C1a	Cre13.g562250	150	60	59	60	66	1.16	1.06	0.99
FAP101	C1a	Cre02.g112100	86	27	27	26	27	1.01	1.04	0.81
FAP119	C1a	Cre06.g256450	34	12	12	13	12	1.13	0.81	0.85
FAP227	C1a	Cre17.g729850	17	17	17	17	16	1.01	0.96	0.91
FAP114	C1a	Cre09.g389282	32	15	14	17	13	0.91	0.79	0.59
FAP81	C1e	Cre06.g296850	172	68	68	73	68	1.07	1.06	1.36
FAP216	C1c	Cre12.g497200	79	33	31	32	31	0.74	0.89	0.87
FAP76	C1c	Cre09.g387689	162	76	82	79	76	1.11	1.02	0.87
Hydin	C2b	Cre01.g025400	528	209	217	227	212	1.06	1.16	1.14
FAP7[a]	?	Cre12.g531800	55	23	24	27	26	1.01	1.24	1.33
FAP47[a]	?	Cre17.g704300	310	120	126	136	123	1.07	1.09	1.34
FAP49[b]	C2	Cre08.g362050	295	35	32	36	40	0.98	1.29	1.22
FAP65[a]	C2	Cre07.g354551	220	69	75	82	69	1.15	1.05	1.54
FAP70[a]	C2	Cre07.g345400	114	41	43	46	42	1.17	1.10	1.36
FAP72[b]	?	Cre08.g362000	595	32	35	33	40	1.36	1.28	1.03
FAP75[a]	C2	Cre06.g249900	125	40	40	38	38	0.91	0.88	1.22
FAP99[a]	C1	Cre14.g624400	90	50	53	58	53	1.22	1.21	0.94
FAP105[a]	C1	Cre12.g511750	31	23	20	24	18	0.74	0.67	0.78
FAP108[a]	C1	Cre06.g297200	22	11	13	12	11	0.93	0.94	0.68
FAP123[a]	?	Cre03.g171800	34	18	19	20	19	0.94	0.79	1.32
FAP125[a]	?	Cre12.g546100	112	62	63	64	68	1.13	1.29	0.82
FAP139[b]	?	Cre09.g387912	76	30	31	34	32	1.04	1.13	1.05
FAP147[a]	C2	Cre04.g224250	97	41	48	40	42	1.43	1.16	1.83
FAP154[b]	?	Cre08.g362100	467	42	52	41	58	1.25	1.36	0.63
FAP171[a]	C2	Cre14.g624900	81	23	22	26	26	0.83	0.87	0.51

FAP174[b]	?	Cre02.g105950	10	6	6	7	5	1.09	0.71	0.81
FAP178[b]	C2	Cre10.g418150	20	6	6	7	5	0.87	0.51	0.60
FAP194[a]	?	Cre12.g522150	52	26	26	27	28	0.95	0.98	1.03
FAP225[a]	?	Cre01.g051050	81	42	45	48	41	1.14	0.88	1.18
FAP239[a]	C2	Cre03.g145387	23	13	15	16	14	1.20	1.12	1.29
FAP266[a]	?	Cre16.g690450	22	5	7	8	5	1.02	0.99	0.94
FAP275[b]	C1	Cre05.g239200	18	10	8	10	8	0.72	0.68	0.97
FAP286[b]	C2	Cre12.g509800	17	11	13	19	9	1.11	0.64	1.26
FAP289[a]	C1	Cre01.g009800	46	19	18	22	20	1.06	1.17	1.09
FAP312[a]	C2	Cre14.g630200	34	41	40	40	39	0.92	0.83	1.06
FAP345[b]	C1	Cre15.g640000	13	29	33	36	31	1.39	1.19	1.30
FAP348[b]	C1	Cre16.g693204	96	35	32	36	35	0.70	1.05	1.58
FAP380[b]	?	Cre01.g010400	20	7	7	7	4	0.53	0.40	0.73
FAP411[b]	C1	Cre09.g409600	13	13	11	12	14	0.82	1.21	1.08
FAP412[a]	C1	Cre12.g497450	57	24	22	24	20	0.85	0.63	0.96
FAP416[b]	?	Cre17.g697750	17	2	2	2	2	1.22	1.27	1.25
DIP13[b]	?	Cre17.g724550	13	10	8	13	8	0.81	0.77	1.58
DPY30[b]	C1	Cre06.g279100	11	5	5	5	4	0.83	0.66	0.73
MOT17[a]	C1	Cre11.g482300	47	23	23	27	21	0.25	0.27	0.58
FAP173[c]	?	Cre16.g690879	33	15	10	11	14	0.25	0.27	0.58
FAP209[c]	C1c	Cre02.g147750	111	43	44	43	47	1.77	1.23	3.87
FAP219[c]	C1c	Cre16.g650450	25	18	17	17	18	0.81	0.88	1.03
FAP244[c]	C2	Cre08.g374700	178	55	56	58	55	1.06	1.01	1.29
FAP279[c]	C1d	Cre06.g268650	30	14	16	18	16	1.12	1.14	0.98
FAP331[c]	C1b/f	Cre06.g308000	205	89	89	88	91	1.04	0.96	1.48
FAP401[c]	C1a/e	Cre12.g529700	101	39	38	38	40	0.88	0.89	1.75

[a]Novel proteins that are predicted to be CA proteins by both (Zhao et al., 2019) and (Dai et al., 2020).

[b]Novel proteins that are predicted to be CA proteins only by (Zhao et al., 2019).

[c]Novel proteins that are predicted to be CA proteins only by (Dai et al., 2020).

Table S2. Exclusive unique FAP246 and FAP413 peptides identified in the proteomic analyses of *fap246* axonemes

Protein	Peptide Sequence	Start residue number	End residue number
FAP246	TADGLKPAYLTLSLTGTDLANADVLGAFPHLQTLVLR	62	98
	SLPPPPPPEPVEEPK	30	44
	PSDGASVAGSSR	2	13
	NALDMLR	151	157
	LTSLSAAHNR	165	174
	LPADGASGPTNLR	132	144
	HLTAVDVSGNK	113	123
	DAFQPSMLSAGLSQLGR	45	61
FAP413	AGLLDLLR	1126	1133
	SLVSGSEDKTLR	1442	1453

Table S3. Exclusive unique FAP42 and FAP413 peptides identified in the proteomic analyses of *fap42* axonemes

Protein	Peptide Sequence	Start residue number	End residue number
FAP42	AALQAAWAAGK	1690	1770
	AQVAGQLVLEAFDWR	1927	1949
	DALYVFVASPGQLR	906	919
	DGSTLVLDPTAQLR	2401	2414
	DLEGSLQAGHR	123	130
	EAEAAAAEAAMK	925	936
	EAISTLSPIIR	510	520
	EFPDVFAYPR	570	579
	EMEAAAAAGSPFDATIVNDDPEAAYAELTR	732	761
	GAGTTAITNAALLR	863	872
	GVNEEGTYCLTVTCTSPLAGAAAGAGALTEVPCHR	2101	2135
	HAVAAVTLVK	286	295
	LALSDAHVAALR	1418	1429
	LHATELPASGAGYCLLALYDTGSR	2077	2100
	LIVLVGPSGVGR	306	317
	LPVVEGPLELALALK	1701	1715
	LRDHLTETDEEIAAR	711	725
	MLLQQLGEQLELVPVVTSRPPLR	1595	1617
	NVLVLAGPAGVGK	1577	1589
	QQLLQLQQDDGR	1489	1500
	REMEAAAAAGSPFDATIVNDDPEAAYAELTR	731	761
	RIDGLYVFVSPPSLDELER	420	438
	RPEELVLNSPDVPMVTTVAPPPPPEPTGGK	72	101
	SCTVLADNALAK	2297	2300
	TLMANAGLLELPR	1958	1968
	VALLYVDSPEPVK	1460	1472
	VLPAGGKPGSGPVLLSAEQLAER	2332	2354

	VPELAVVPSTSLK	1379	1391
	YGEAPAGAVGVLFR	1935	1948
FAP413	VQPAAAAAYEAQDDLR	423	438
	VLDSVASSSEALQELQPR	94	111
	SVVSGSLDSTLR	1791	1802
	SLVEGVGDTLAR	328	339
	LPLSQAFEWLLEAPLNR	923	939
	INVVSSVCFSPDGR	1643	1456
	FGAGSWLR	373	380
	DLEGPLAGLTAHLR	351	364
	ASAEATKPNQQQR	14	26
	APTGTAVFQEAR	1377	1388

Table S4. Primers used in this study to confirm the mutant insertion site

Name	Sequence (5'-3')	Sequence (3'-5')
fap246	TGTTGTGCCGCGCCTGCGAG	TCTTGGCTCAGCGGCTCTTG
fap413	ACATTGCCCTCAACAAGACC	TGATAGGACTCGGGATGGAG
fap42	GCCTACCTGTTCATTGGCAT	GCCTACCTGTTCATTGGCAT

Table S5. Summary of image processing information for the strains used in this study

Strains	**Number of Tomograms**	**Number of averaged CA repeats**	**Resolution (nm)**	**TEM/Camera**
WT	14	664	2.3	Krios/K2/VPP
fap246	38	1633	2.2	Krios/K3/VPP
fap413	30	1401	2.5	Krios/K3/VPP
fap42	25	1142	2.5	Krios/K3/VPP

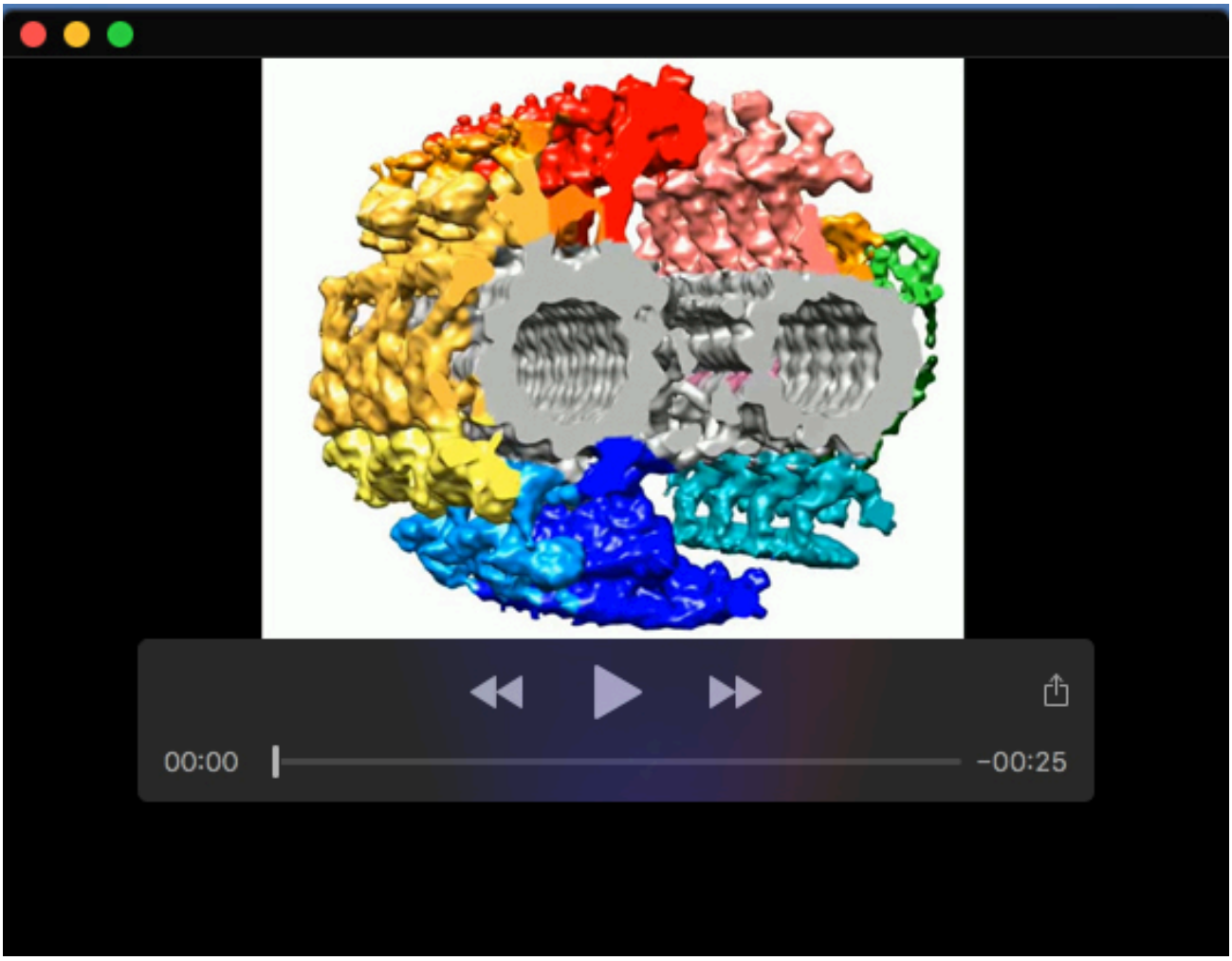

Movie 1. Animated 3D visualization of the averaged repeats of the *Chlamydomonas* WT CA. The averaged CA repeats are shown in cross-sectional orientation at the beginning of the animation. The CA projections associated with the C1 and C2 microtubules are indicated (nomenclature and color coding follow that of (Carbajal-Gonzalez et al., 2013) and (Fu et al., 2019)).

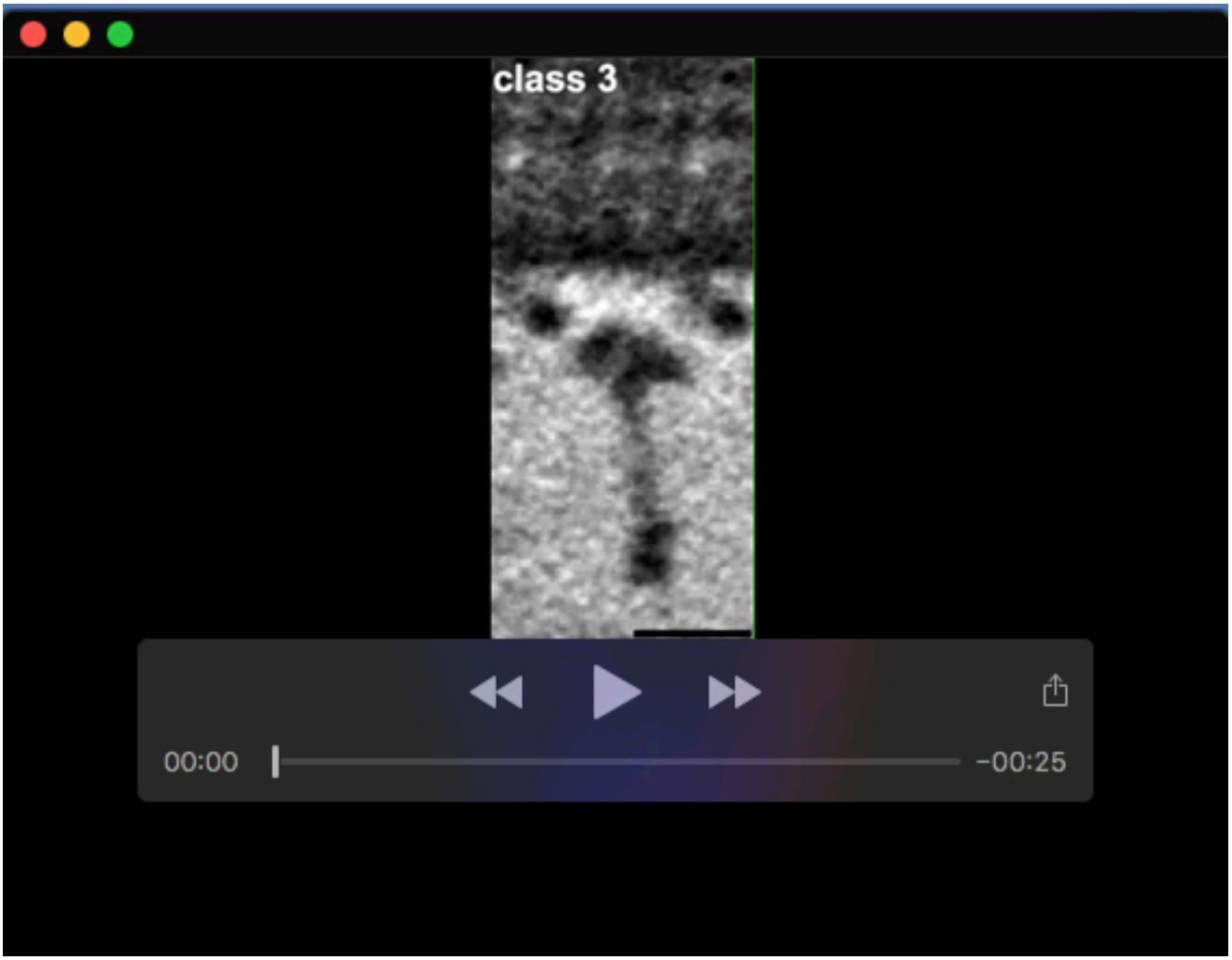

Movie 2. Comparison of the four class averages of the *fap246* CA shows positional flexibility of the C1b projection. Sequence of one tomographic slice for each class average in longitudinal orientation. Related to Fig. 2. Scale bar: 10 nm.

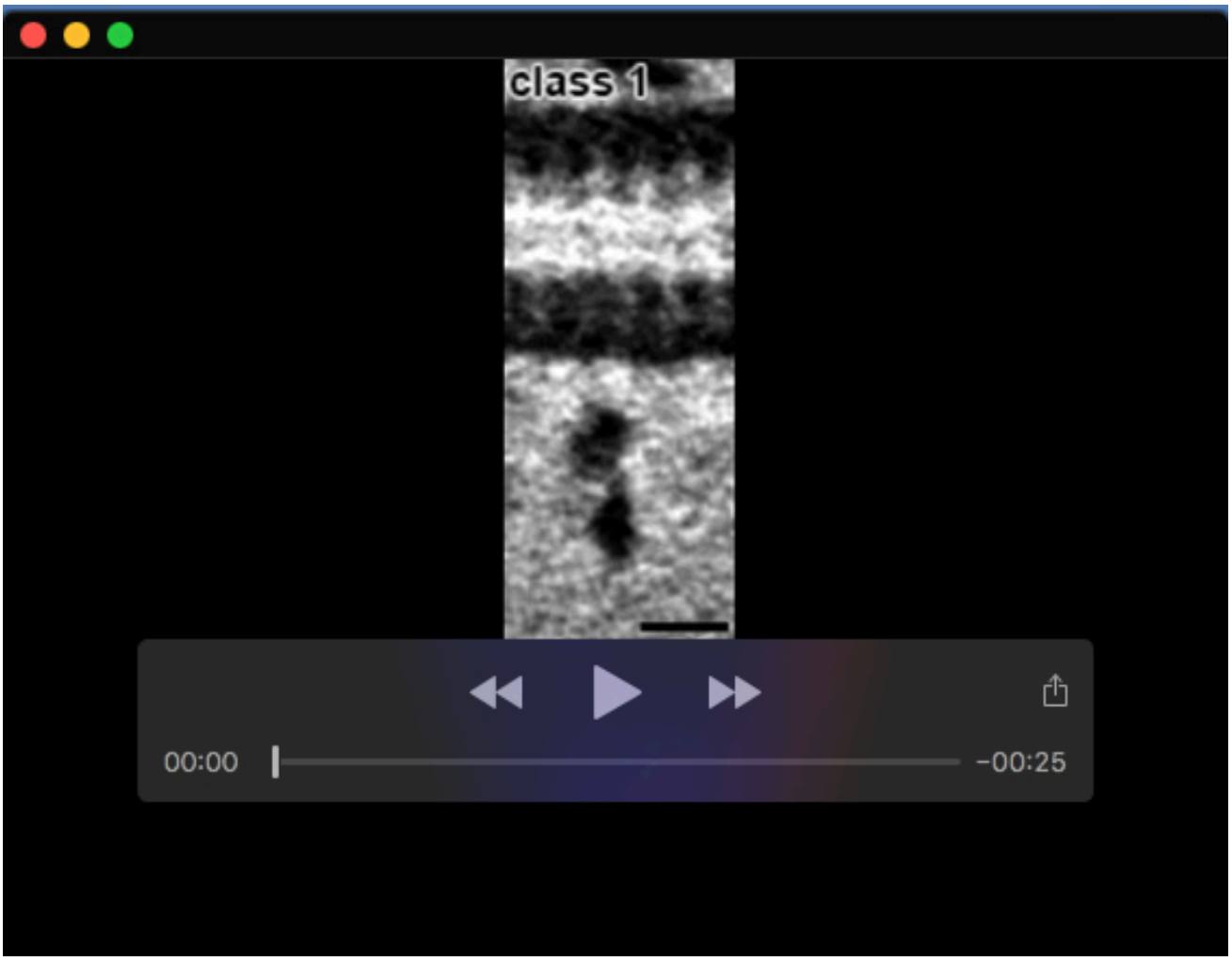

Movie 3. Comparison of the three class averages of the *fap42* CA shows positional flexibility of the C1f projection. Sequence of one tomographic slice for each class average in longitudinal orientation. Related to Fig. 4. Scale bar: 10 nm.

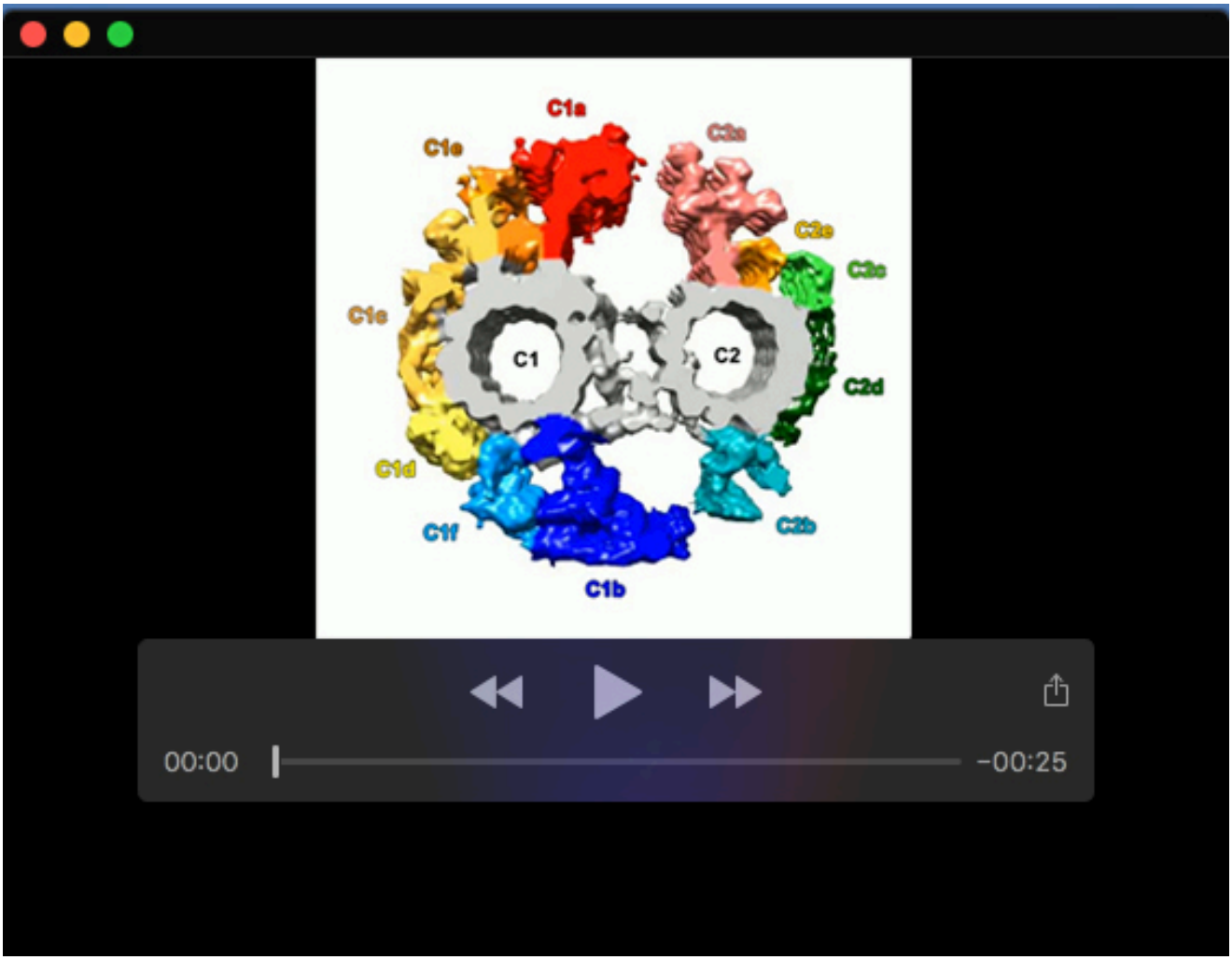

Movie 4. Animated 3D visualization of the averaged repeats of the *Chlamydomonas* WT CA highlighting the locations of FAP246, FAP413, and FAP42 within the C1b projection. Nomenclature and color coding of the CA projections are indicated.

Supplementary References:

Carbajal-Gonzalez, B. I., Heuser, T., Fu, X., Lin, J., Smith, B. W., Mitchell, D. R. and Nicastro, D. (2013). Conserved structural motifs in the central pair complex of eukaryotic flagella. *Cytoskeleton (Hoboken)* **70**, 101-120.

Dai, D., Ichikawa, M., Peri, K., Rebinsky, R. and Bui, K. (2020). Identification and mapping of central pair proteins by proteomic analysis. *Biophysics and Physicobiology* **17** 71-85.

Fu, G., Zhao, L., Dymek, E., Hou, Y., Song, K., Phan, N., Shang, Z., Smith, E. F., Witman, G. B. and Nicastro, D. (2019). Structural organization of the C1a-e-c supercomplex within the ciliary central apparatus. *J Cell Biol* **218**, 4236-4251.

Hoops, H. J. and Witman, G. B. (1983). Outer doublet heterogeneity reveals structural polarity related to beat direction in Chlamydomonas flagella. *J Cell Biol* **97**, 902-8.

Lindemann, C. B. and Mitchell, D. R. (2007). Evidence for axonemal distortion during the flagellar beat of Chlamydomonas. *Cell Motil Cytoskeleton* **64**, 580-9.

Mitchell, D. R. (2003). Orientation of the central pair complex during flagellar bend formation in Chlamydomonas. *Cell Motil Cytoskeleton* **56**, 120-9.

Zhao, L., Hou, Y., Picariello, T., Craige, B. and Witman, G. B. (2019). Proteome of the central apparatus of a ciliary axoneme. *J Cell Biol* **218**, 2051-2070.